Functional expansion of the Anderson and SU(N) models

M. E. Foglio
Instituto de Física "Gleb Wataghin," Universidade Estadual de Campinas, 13081, Campinas, São Paulo, Brasil
(Received 11 May 1990; revised manuscript received 10 September 1990)

We study the Anderson and SU(N) lattice models that describe the Kondo and intermediate-valence systems, in the infinite-correlation limit ($U \to \infty$), employing the functional expansion. We use Hubbard operators that describe real electrons. In the lowest, nontrivial approximation, our expressions are similar to, but different from, those derived by several effective-Hamiltonian techniques, like the mean-field slave-boson (MFSB) technique. In the usual large-N limit, our results coincide with those of the equations of motion and Brillouin-Wigner expansions, which are exact in that limit. Our results at $T=0$ K are compared to those of the MFSB quasiparticle description, and we discuss the two approximations in the region in which they are different. We conclude that although the quasiparticle description should give better results for the thermodynamic properties, our treatment describes in a more physical way the overall behavior of the spectral density of the localized electrons. The structure near the chemical potential that is predicted in other methods is not obtained in our treatment, but I believe that it would appear if a higher-order approximation were employed.

I. INTRODUCTION

The study of heavy-fermion systems and high-T_c superconductivity has shown the importance of considering the strong correlations between electrons for an understanding of these recently discovered phenomena. Exact solutions are only known for a few limiting cases that do not correspond to most situations of interest, and it is essential to develop techniques for deriving adequate approximations. The limit of a narrow band was discussed in a series of papers by Hubbard,[1] and he introduced a deceptively simple Hamiltonian to study the strong local correlation between electrons at the same site. To describe the electronic states, he employed the X operators, which are very adequate to study atomic states: $X_{j\alpha\beta}=|j\alpha\rangle\langle j\beta|$ transforms the local state β into the state α, both at site j. Their use makes it possible to include strong local correlations in an extremely simple Hamiltonian that has only the hopping term. These X operators are not fermions or bosons, so that Wick's theorem is not valid, and the first treatments of the problem were made by decoupling the Green's-function (GF) equations of motion. Besides problems with the violation of spectral sum rules in this method, the choice of the decouplings is rather arbitrary, and one would like a more systematic method; but we should mention a recent decoupling technique[2] employed for the Anderson model that seems rather promising.

Several methods have been used to study the Anderson model: Let us mention (a) perturbation expansion with X operators,[3] (b) the Gutzwiller variational technique,[4] and (c) slave-boson methods.[5] In these techniques one can use the large-N approximation,[6] based in the SU(N) model, which is a natural extension of the Anderson model: The Hamiltonian has N rather than only two channels for both the localized and conduction electrons, with hybridization allowed only within each of the channels. An exact solution is obtained by taking $N \to \infty$ and keeping $NV^2=$const (where V is the hybridization constant) and the expansion is made about this limit with $1/N$ as a parameter. In method (c) an auxiliary boson field is added to the Fermi field, and the correlation is forced on the system by local constraints: The operators in the Hamiltonian are true fermions and bosons, and Wick's theorem is satisfied. Both standard perturbation expansions and functional integral methods have been employed to study the slave-boson Hamiltonian, but in the lowest approximation one can use[7] a rather simple mean-field slave-boson (MFSB) method. In both the Gutzwiller and MFSB approximations, the system is described by an effective Hamiltonian, describing two hybridized bands with renormalized localized energy $\tilde{E}$ and hybridization parameter $\tilde{V}$. There are small but important differences in the two results, but it has been recently shown[8] that a modification of the MFSB treatment gives coincident results. In a recent paper[9] the functional technique employed by Kadanoff and Baym[10] (KB) to expand GF was applied by Ruckenstein and Schimtt-Rink[9] (RS) to study the Hubbard model. This method seemed to be particularly suitable for our purposes, because it shows how to obtain in a systematic way approximations that conserve several important quantities.

In the present paper we shall study the Anderson model in the $U \to \infty$ limit employing the KB technique. The simplest nontrivial result is the analog of the Hartree-Fock approximation, but applied to a self-energy term and not to the U term of the Hubbard Hamiltonian: This last approximation would have no sense in the $U \to \infty$ limit. It seemed interesting to compare our results with those of the MFSB approximation for arbitrary N, and we studied the SU(N) model, which includes the Anderson model for $N=2$. The results we find employing the KB expansion in the IV region are qualitatively similar to those obtained by the "effective Hamiltonian" methods

discussed above, but they are rather different in the Kondo region. To give a unified picture of these conflicting results, we have compared them with those obtained by the variational treatment of Brandow.[11] This technique has the advantage of being variational, as the effective Hamiltonians are, and at the same time using a variational wave function with the f^2 configuration automatically empty, so that electronic correlations are satisfied without having to enforce them by extra conditions at the end of the calculation. This analysis leads us to believe that the KB and MFSB treatments show complementary aspects of the system in the Kondo region, each one describing a different spectral region of the f spectral density.

In Sec. II we apply to the SU(N) model the derivation recently employed by RS to study the Hubbard model. In Sec. III we consider in detail a particular model that can be calculated analytically at $T=0$ K and compare the results with those of the MFSB method for the same system. In Sec. IV we consider the apparent discrepancy between our results and those of RS, who state that the KB and MFSB methods give the same results in the $N\rightarrow\infty$ limit. In Sec. V we analyze the results obtained with the KB method, giving particular attention to those that seem to contradict the currently accepted picture.

II. FUNCTIONAL EXPANSION FOR THE SU(N) MODEL

As the techniques employed in this section follow the method[10] of KB employed[9] by RS for the Hubbard model, we shall only give the main steps of the derivation, to show the necessary differences to treat the SU(N) model. As usual, we write the model Hamiltonian as $H=H_0+H'$, with

$$H_0=\sum_{j,\sigma}E(fj\sigma)X_{j,\sigma\sigma}+\sum_{\mathbf{k},\sigma}E(\mathbf{k}\sigma)C^{\dagger}_{\mathbf{k}\sigma}C_{\mathbf{k}\sigma}\ ,$$
$$H'=\sum_{j,\mathbf{k},\sigma}V_{j\mathbf{k}\sigma}X^{\dagger}_{j,0\sigma}C_{\mathbf{k}\sigma}+\text{H.c.} \tag{1}$$

To exclude multiple occupancy of f electrons at each site, we have used the Hubbard operators mentioned in the Introduction. The only localized states at site j are $|j0\rangle$ (no f electron) and the N states $|j\sigma\rangle$ (one f electron in channel σ): All the $X_{j,\alpha\beta}$ operators that appear in our model, besides their specific action, project out from any local state at site j the components with more than one electron at that site. The $C_{\mathbf{k}\sigma}$ are the usual Fermi operators of the conduction band.

To write more compact expressions, we introduce a vector $\mathbf{Y}$ with components $Y(\gamma,\sigma)$ that describes both $X_{j,0\sigma}$ ($\gamma=f,j$) and conduction-electron operators $C_{\mathbf{k}\sigma}$ ($\gamma=c,\mathbf{k}$) as well as the vector $\overline{\mathbf{Y}}$, with components $Y^{\dagger}(\gamma,\sigma)$. The Hamiltonian then reads

$$H=\overline{\mathbf{Y}}\cdot\mathbf{E}\cdot\mathbf{Y}+\overline{\mathbf{Y}}\cdot\mathbf{V}\cdot\mathbf{Y}\ , \tag{2}$$

where the matrix $\mathbf{E}$ is diagonal with components $E(\gamma,\sigma)$ and those of $\mathbf{V}$ are $V(fj\sigma,fj'\sigma')=V(c\mathbf{k}\sigma,c\mathbf{k}'\sigma')=0$ and

$$V(fj,\sigma,c\mathbf{k}\sigma')=V^{*}(c\mathbf{k}\sigma',fj\sigma)$$
$$=V_{j\mathbf{k}\sigma'}\delta_{\sigma,\sigma'}=V/\sqrt{N_s}\exp(i\mathbf{k}\cdot\mathbf{R}_j)\ ,$$

where N_S is the number of sites. To define the imaginary time GF, we introduce $A(\tau)=\exp(\tau H)A\exp(-\tau H)$ and $\overline{A}(\tau)=\exp(\tau H)A^{\dagger}\exp(-\tau H)$. Following KB,[10] it is convenient to introduce an external potential $\mathbf{U}(\tau)$ with components $U_{\sigma\sigma'}(\gamma,\tau),\delta_{\gamma,\gamma'}$ and define the $\mathbf{U}$-dependent GF:

$$G(1,2;\mathbf{U})=-\langle(S(\mathbf{U})Y(1)\overline{Y}(2))_{+}\rangle/\langle S(\mathbf{U})\rangle\ , \tag{3}$$

where we abbreviate $Y(1)=Y(\gamma_1\sigma_1\tau_1)$:

$$S(\mathbf{U})=\exp_{+}\left[\int_0^{\beta}d\tau\,\overline{\mathbf{Y}}(\tau)\cdot\mathbf{U}(\tau)\cdot\mathbf{Y}(\tau)\right]\ . \tag{4}$$

$\beta=1/kT$ and the subindex $+$ indicates τ ordering to the left. We introduce the matrix $\mathbf{G}(\tau_1,\tau_2)$ with components $G(1,2;\mathbf{U})$, and we shall leave the $\mathbf{U}$ implicit unless necessary for clarity. The equation of motion of $\mathbf{G}$ can be put in the form

$$\left[\frac{\partial}{\partial\tau}+\mathbf{E}+\mathbf{V}-\mathbf{U}\right]\mathbf{G}(\tau,\tau')$$
$$=-\mathbf{Q}(\tau)\delta(\tau-\tau')-\int_0^{\beta}d\tau_1\Sigma(\tau,\tau_1)\mathbf{G}(\tau_1,\tau')\ , \tag{5}$$

where the matrix

$$\mathbf{Q}(\tau)=\langle(S(\mathbf{U})\{\mathbf{Y}(\tau);\overline{\mathbf{Y}}(\tau)\})_{+}\rangle/\langle S(\mathbf{U})\rangle \tag{6}$$

is diagonal in γ and symmetric in the σ indices because of the anticommutator $\{\,;\,\}$. The self-energy matrix $\Sigma(\tau,\tau')$

$$\Sigma(\tau,\tau')=\mathbf{P}^{f}\mathbf{A}(\tau)\mathbf{V}\delta(\tau-\tau')$$
$$+\int_0^{\beta}d\tau_1\mathbf{G}^{s}(\tau,\tau_1)\mathbf{G}^{-1}(\tau_1,\tau')\ , \tag{7}$$

where the inverse of $\mathbf{G}(\tau,\tau')$ is defined by

$$\int_0^{\beta}d\tau_1\mathbf{G}^{-1}(\tau,\tau_1)\cdot\mathbf{G}(\tau_1,\tau')=\delta(\tau-\tau')\mathbf{I}\ ,$$

and $\mathbf{I}$ is the identity matrix. The matrix $\mathbf{P}^{f}$ projects on the subspace of f operators:

$$\mathbf{P}^{f}(\gamma\sigma,\gamma'\sigma')\begin{cases}\delta_{\gamma\gamma'}\delta_{\sigma\sigma'} & \text{for } \gamma=(f,j)\ ,\\ 0 & \text{for } \gamma,\gamma'=(c,\mathbf{k}),\end{cases} \tag{8}$$

$$[\mathbf{A}(\tau)]_{\gamma\sigma,\gamma'\sigma'}=\delta_{\gamma\gamma'}\left[G(\gamma\sigma\tau,\gamma\sigma'\tau^{+})-\delta_{\sigma\sigma'}\sum_{s}G(\gamma s\tau,\gamma s\tau^{+})\right]\ , \tag{9}$$

and the components of $\mathbf{G}^{s}(\tau,\tau')$ are

$$G^{s}(\gamma\sigma\tau,\gamma'\sigma'\tau')=\sum_{s'}\left[[\delta/\delta U_{s'\sigma}(\gamma\tau)]-\delta_{s'\sigma}\sum_{s}[\delta/\delta U_{ss}(\gamma\tau)]\right]$$
$$\times[\mathbf{P}^{f}\cdot\mathbf{V}\cdot\mathbf{G}(\tau,\tau',\mathbf{U})]_{\gamma s',\gamma'\sigma'}\ . \tag{10}$$

Although one does not know how to solve equations with functional derivatives $\delta/\delta U$, they provide a systematic procedure to obtain "conserving" expansions[10] for the GF. Employing $\mathbf{G}^{-1}(\tau,\tau')$ and the inverse of $\mathbf{Q}(\tau)$ at a

given τ [i.e., $\mathbf{Q}(\tau)\cdot\mathbf{Q}^{-1}(\tau)=\mathbf{I}$], one can express $\mathbf{G}^s(\tau,\tau')$ as a function of functional derivatives $\delta\mathbf{Q}(\tau)/\delta U$ and $\delta\Sigma(\tau,\tau')/\delta U$. The lowest-order approximation neglects these two functional derivatives: This corresponds to a Hartree-Fock approximation for $\Sigma(\tau,\tau')$. Taking $U=0$, Eq. (1) commutes with the spin components, and $\mathbf{G}$, $\mathbf{Q}$, and $\mathbf{G}^s$ are then diagonal in the spin index σ: so we denote their diagonal elements with $G(\sigma;\gamma\tau,\gamma'\tau')$, $Q(\sigma;\gamma\tau)$, and $G^s(\sigma;\gamma\tau,\gamma',\tau')$. We obtain, in this approximation,

$$G^s(\sigma;fj\tau,\gamma'\tau')=\sum_{\mathbf{k}}\left[\sum_{s\neq\sigma}VG(s;c\mathbf{k}\tau,fj\tau)Q^{-1}(s;fj)\right]G(\sigma;fj\tau,\gamma'\tau')\ , \tag{11}$$

$$G^s(\sigma;c\mathbf{k}\tau,\gamma'\tau')=0$$

(cf. the presence of $\mathbf{P}^f$ in $\mathbf{G}^s$). Because of the invariance against time translation of the Hamiltonian

$$\mathbf{G}(\tau,\tau')=\mathbf{G}(\tau-\tau')\ ,$$

we define the Fourier transform

$$\mathbf{G}(\omega_\nu)=\int_0^\beta\mathbf{G}(\tau,\tau')\exp[i\omega_\nu(\tau-\tau')]d\tau$$

with $\omega_\nu=(2\nu+1)\pi/\beta$, where ν is an integer. For a uniform system,

$$\begin{aligned}
&G(\sigma;c\mathbf{k},c\mathbf{k}'/\omega_\nu)=\delta_{\mathbf{k}\mathbf{k}'}/(i\omega_\nu-\tilde{E})/\Delta(\mathbf{k},i\omega_\nu)\ ,\\
&G(\sigma;f\mathbf{k},f\mathbf{k}'/\omega_\nu)=\delta_{\mathbf{k}\mathbf{k}'}[i\omega_\nu-E(\mathbf{k}\sigma)]Q_\sigma/\Delta(\mathbf{k},i\omega_\nu)\ ,\\
&G(\sigma;c\mathbf{k},f\mathbf{k}'/\omega_\nu)=\delta_{\mathbf{k}\mathbf{k}'}V^*Q_\sigma/\Delta(\mathbf{k},i\omega_\nu)\ ,\\
&G(\sigma;f\mathbf{k},c\mathbf{k}'/\omega_\nu)=\delta_{\mathbf{k}\mathbf{k}'}(1-(N-1)\langle X_{ss}\rangle)V/\Delta(\mathbf{k},i\omega_\nu)\ ,
\end{aligned} \tag{12}$$

where

$$\Delta(\mathbf{k},z)=(z-\tilde{E})\cdot[z-E(\mathbf{k}\sigma)]-|\tilde{V}|^2\ , \tag{13}$$

$$\tilde{E}=E(f\sigma)-VQ_\sigma^{-1}\sum_{s\neq\sigma}\langle X_{0s}^\dagger(j)C_{js}\rangle\ , \tag{14}$$

$$Q_\sigma=\langle X_{00}\rangle+\langle X_{\sigma\sigma}\rangle, \tag{15}$$

$$|\tilde{V}|^2=(1-\sum_{s\neq\sigma}\langle X_{ss}\rangle)|V|^2\ , \tag{16}$$

and $\langle X_{ss}\rangle\equiv\langle X_{j,ss}\rangle$ is independent of j.

The operator $C_{j\sigma}$ destroys an electron in the Wannier state at site j, and in the uniform case all properties are independent of the site. In the paramagnetic case the $\sum_{s\neq\sigma}$ becomes $N-1$ because the properties are independent of the spin component and the calculation is simpler.

The GF's in Eqs. (12)–(16) have poles at the solutions $\omega_\alpha(\mathbf{k})$ ($\alpha=1.2$) of $\Delta(\mathbf{k},z)=0$. They correspond to the dispersion relations of a band $E(\mathbf{k}\sigma)$ and a lattice of localized f electrons with energy $\tilde{E}$ hybridized with a constant $\tilde{V}$. The local spectral density of f electrons per channel is

$$\rho^f(\omega)=(1/N_s)\sum_{\mathbf{k}}(-1/\pi)\mathrm{Im}G(\sigma;f\mathbf{k},f\mathbf{k}/-i(\omega+i0)) \tag{17}$$

It is clear that if the general property of GF, $G^*_{AB}(z)=G_{B^\dagger A^\dagger}(z^*)$ is satisfied, one must have $Q_\sigma=1-\sum_{s\neq\sigma}\langle X_{ss}\rangle$, which is also consistent with the local completeness $X_{00}+\sum_\sigma X_{\sigma\sigma}=I$, in this case, $|\tilde{V}|^2=Q_\sigma|V|^2$.

III. RESULTS FOR A SIMPLE MODEL

We present here results for $T=0$ K taking a rectangular conduction band of width $2D$ and centered at the origin (i.e., a density of states per channel $\rho^0=1/2D$). Each "band" $\omega_\alpha(\mathbf{k})$ is in the interval $[\omega_{\alpha m},\omega_{\alpha M}]$, where

$$\begin{aligned}
2\omega_{\alpha m}&=\tilde{E}-D\pm[(D+\tilde{E})^2+4\tilde{V}^2]^{1/2}\ ,\\
2\omega_{\alpha M}&=\tilde{E}+D\pm[(D-\tilde{E})^2+4\tilde{V}^2]^{1/2}\ .
\end{aligned} \tag{18}$$

The $\alpha=1$ (2) corresponds to the $+$ ($-$) sign and is therefore the upper (lower) "band"; the effective $\tilde{E}$ is always in the gap. The local spectral density of f electrons in the model is

$$\rho^f(\omega)=\rho^0Q\tilde{V}^2/(\omega-\tilde{E})^2\ . \tag{19}$$

We give here results valid for the chemical potential μ inside the lower "band"; similar results hold in the other cases:

$$\begin{aligned}
&\tilde{E}=E_f+(N-1)|V|^2\rho^0\ln[(\tilde{E}-\omega_{2m})/(\tilde{E}-\mu)]>0\ ,\\
&n^\sigma=Q\rho^0|\tilde{V}|^2\{[1/(\tilde{E}-\mu)]-[1/(\tilde{E}-\omega_{2m})]\}\ ,\\
&n^c=\rho^0(\mu-\omega_{2m})\ ,
\end{aligned} \tag{20}$$

where n^c and n^σ are, respectively, the number of conduction and f electrons per channel per site, and we write $E_f=E(f)$ for convenience. In the $N\to\infty$ limit these expressions are exactly those derived in several "effective Hamiltonian" treatments[12] [cf. Eqs. (70), (72), and (74) in Ref. 7], except that our expression for n^α has an extra factor Q and we have $(N-1)$ instead of N in $\tilde{E}$. This reflects the fact that the effective $\tilde{H}$ in those works describe two hybridized bands without correlation and with an integrated f spectral density per channel equal to 1, while in our case the spectral density integrates to $Q<1$ because of the f-electron local correlation. In the effective Hamiltonian treatments, the correlation is forced on the model through extra conditions, and the resulting $\tilde{E}$ is slightly above μ when $E_f<\mu$ so that the energy renormalization $\tilde{E}-E_f\sim\mu-E_f$ when E_f is rather below μ. The uncorrelated fermions that appear in $\tilde{H}$ describe quasiparticles, while the X operators in our GF correspond to correlated f electrons and do not require

extra conditions to keep the total number of electrons per site less than 1. The X operators are not Fermion operators because the double occupancy has been projected out, and one should not try to force them to have the full spectral weight of the f electrons. In the large-N limit (keeping NV^2 constant), our f-electron GF tends to a δ function at $\tilde{E}$ with strength Q, which is the exact solution in this limit.[13]

It is interesting to compare the results of the two types of treatments for specific values of the parameters: We shall keep V and the total number of electrons constant, and plot the chemical potential μ, the difference $\tilde{E}-\mu$, the total number of f electrons $n^f=Nn^\sigma$, and the f local spectral density at the Fermi surface $\rho^F=\rho^f(\mu)$ as a function of the unrenormalized f-electron energy E_f. From the practical point of view, it is easier to start from given $\tilde{E}$, V, and $\langle X_{\sigma\sigma}\rangle$, take $Q=1-(N-1)\langle X_{\sigma\sigma}\rangle$, and calculate $\tilde{V}$ from Eq. (16); the value of μ that gives $\langle X_{\sigma\sigma}\rangle$ is then easily obtained. The f spectral density derived from Eq. (12) always integrates to Q, and from this invariance it follows that $\langle X_{00}\rangle=Q-\langle X_{\sigma\sigma}\rangle=1-N\langle X_{\sigma\sigma}\rangle$, so that the local completeness is automatically satisfied. The unrenormalized E_f and n^c are obtained from Eqs. (18), and the total number of electrons per channel is $n^t=n^c+n^\alpha$; a unique solution is obtained by this procedure, and the value of μ that gives the n^t we want is obtained by varying the starting $\langle X_{\sigma\sigma}\rangle$; one can then plot the different parameters as a function of E_f. In a similar way we study the MFSB approximation,[7] but for given n^t and sufficiently low $\tilde{E}$ there is no solution: In this case we employ the usual method to obtain $\tilde{E}$ as a function of E_f.

In Fig. 1(a) we plot $\tilde{E}-\mu$ and μ as a function of E_f for $V=0.3$, $D=10$, $N=2$, $T=0$ K, and $n^t=0.5$. Here and in what follows we employ the same energy unit in all parameters and variables, so that the unit of ρ^f is the inverse of the energy unit: The results are then invariant against a change of the energy unit. The two graphs of $\tilde{E}-\mu$ and μ are indistinguishable, except that in the MFSB technique the μ (dashed line) remains near the bottom of the conduction band when E_f goes below that value: As discussed above, this is necessary to keep $n^f<1$. In our calculation (KB) both $\tilde{E}$ and μ keep decreasing for $E_f<D$, giving again $\tilde{E}-\mu\sim 0$. In Fig. 1(b) we show ρ^F, the spectral density at μ for both KB (solid line) and MFSB (dotted line) methods, as well as the total number n^f of f electrons (dashed line). It is then clear that the properties that depend on ρ^F at μ would be at least qualitatively similar for the two methods in the region of interest (i.e., E_f inside the conduction band). This type of behavior is repeated for $n^t<0.5$.

The situation is qualitatively different for $n^t>0.5$, as shown in Figs. 1(c) and 1(d) for the same parameters, but for $n^t=0.75$ (not the different scales employed for $n^t=0.5$). The two graphs of μ are indistinguishable in Fig. 2(a), but the $\tilde{E}-\mu$ are different below a given energy E_f as was discussed before. The plot shows that for the KB method there is an interval of E_f in which $\tilde{E}-\mu$ is very close to zero, and this region coincides with the interval in which μ increases from one plateau to a higher one. The interpretation is clear: This is the interval in

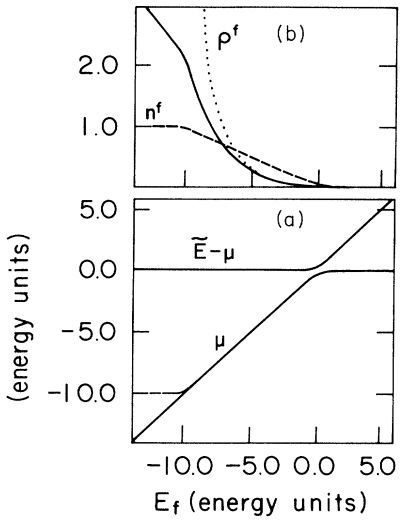

FIG. 1. Parameters and units employed are discussed in the text. (a) Chemical potential μ and $\tilde{E}-\mu$ are plotted as a function of the unrenormalized f energy E_f for both the KB and MFSB methods. For $E_f<10$ the two μ curves are different, the solid line corresponds to the KB method. The two $\tilde{E}-\mu$ curves cannot be distinguished in the plot. (b) The total number of f electrons $n^f=Nn^\sigma$ (dashed line) and the f spectral densities ρ^f at μ are plotted as a function of E_f for the MSFB method (dotted line) and for the KB method (solid line). The two ρ^f have been multiplied by 0.005 to fit the vertical scale.

which the f electrons are transferred into the conduction band as E_f increases, and this is shown in Fig. 2(b), where n^σ and ρ^F are plotted against E_f for the two methods. The KB value of ρ^F has a sharp maximum in this interval, and we expect that the model would predict heavy-fermion (HF) properties for the system in this region; inside this interval there is a smaller one in which $E<\mu<\tilde{E}$.

The KB spectral density in Fig. 2(b) is not monotonic as in Fig. 1(b), but shows a very asymmetric peak. The meaning of this asymmetry is traced back to the jump of μ from the upper band into the lower band: When E_f increases, the number of conduction-band electrons also increases and n^f decreases, as shown in the figure, until a point in which the number of f electrons in the lower band is enough to give the required $n^t=n^f+n^c$. This behavior cannot be present in the MFSB treatment because μ is always in the lower band to keep $n^f<1$.

Figures 2–4 are the same as Figs. 1 and 2, but with $N=10$. The same qualitative features are observed as in Figs. 2(a) and 2(b), but the interval in which $\tilde{E}-\mu\sim 0$ is rather smaller than in Fig. 2: This is because the maximum number of f electrons per channel is $1/N$, and they are all transferred to the conduction band in a smaller interval of E_f when N increases (we have not plotted the MFSB value of ρ^F in this figure for clarity). A behavior similar to that of Fig. 1(b) would only occur for $Nn^t<1$.

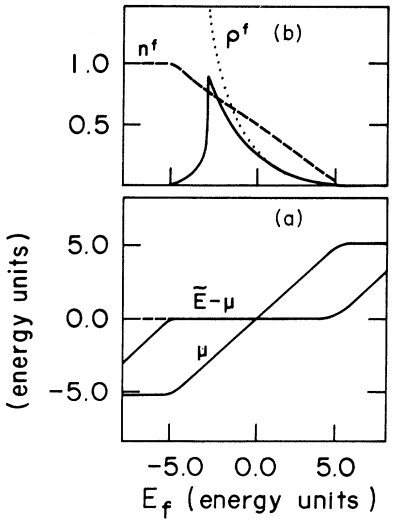

FIG. 2. (a) Same plot as Fig. 1(a), but for $n^f=0.75$. Here the two curves of $\tilde{E}-\mu$ are different for E_f below -5 (the dashed line corresponds to the MFSB method). Note the different scale than in Fig. 1(a). (b) Same plot as Fig. 1(b), but for $n^f=0.75$. Note again the different scales.

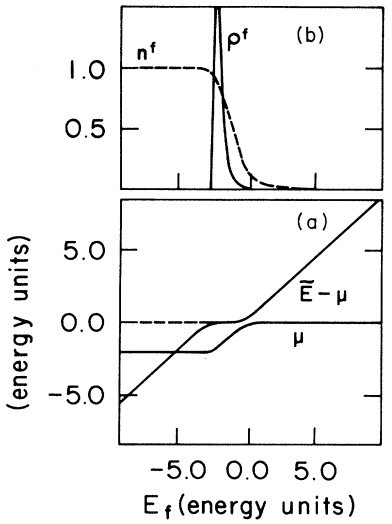

FIG. 3. All the parameters and curves correspond to those of Fig. 1, but for $N=10$.

IV. FUNCTIONAL EXPANSION AND THE HUBBARD MODEL

A very important point is the apparent discrepancy between our results and those derived by RS for the Hubbard model. They state that their results agree with those of the MFSB method in the $N\to\infty$ limit, while for the Anderson model we have found that the KB and MFSB methods give rather different results, particularly in the Kondo limit. To study this problem we repeated the calculations for the Hubbard model with the same approximations we have used for the Anderson model. For infinite correlation (i.e., $U\to\infty$), we write the Hubbard Hamiltonian as

$$H=-\sum_{\sigma}\sum_{i,j} t_{ij}X^{\dagger}_{i,0\sigma}X_{j,0\sigma} , \tag{21}$$

where we assume that $t_{jj}=0$ and $\sigma=1,2,\ldots,N$ (i.e., there are N channels). The derivation follows the same steps as before, and the lowest nontrivial approximation takes all the $\delta\Sigma/\delta U=\delta Q/\delta U=0$. When the external potential U is zero and the system is paramagnetic, we can Fourier transform in space and imaginary time. One then easily finds the GF:

$$G_{\mathbf{k}\sigma}(z)=Q/\{z-[\tilde{E}(\mathbf{k})+\tilde{E}_0]\} , \tag{22}$$

where

$$\tilde{E}(\mathbf{k})=Q\sum_i(-t_{ij})\exp[-i\mathbf{k}\cdot(\mathbf{R}_j-\mathbf{R}_i)] , \tag{23}$$

$$Q\tilde{E}_0=-(N-1)\sum_i(-t_{ij})\langle X^{\dagger}_{j,0\sigma}X_{i,0\sigma}\rangle , \tag{24}$$

and

$$Q=1-n^f+n^f/N . \tag{25}$$

As a simple model, we assume that in the absence of correlation (i.e., no f-f repulsion) we have a rectangular band centered at the origin and with a half-width $2D$ (i.e., a density $\rho^0=1/2D$ per channel). Equation (22) is proportional to the GF of a band centered at $\tilde{E}_0$ and with a half-width of $\tilde{D}=QD$ (the constant of proportionality is Q). Following standard methods, we find

$$n^f=Q(N/2\tilde{D})(\mu-\tilde{E}_0+\tilde{D}) , \tag{26}$$

and

$$Q\tilde{E}_0=-[(N-1)/2\tilde{D}][(\tilde{E}_0-\mu)^2/2-(\tilde{D})^2/2] . \tag{27}$$

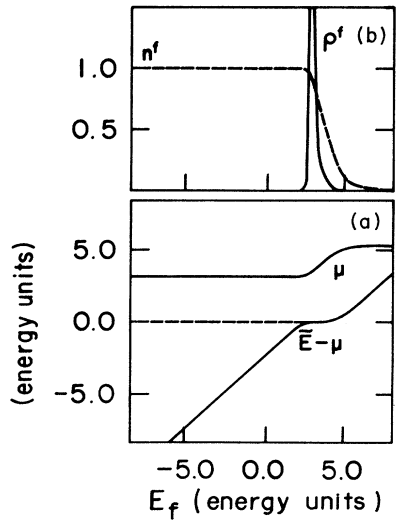

FIG. 4. All the parameters and curves correspond to those of Fig. 2, but for $N=10$.

To compare with the MFSB results, we shall denote with a prime the quantities that in the MFSB method correspond to the unprimed unities of the KB, e.g., we shall use $\tilde{E}'_0$, Q', etc., instead of $\tilde{E}_0$, Q, etc. In the MFSB method Eqs. (26) and (27) are valid, but with the following differences: The Q factor is missing in Eq. (26), there is an N rather than $N-1$ in $\tilde{E}'_0$ [cf. Eq. (27)], and instead of Eq. (25) we have $Q'=1-n^f$ [cf. Eqs. (119), and (120) in Ref. 7]. These are the same differences we have obtained for the Anderson model, and one would naively expect that different results would be again obtained, even in the limit of $N\to\infty$.

From Eqs. (26) and (27), one finds

$$Q\tilde{E}_0=(1-1/N)Dn^f(1-n^f)\ , \tag{28}$$

while for the MFSB method we obtain

$$\tilde{E}'_0=Dn^f(1-n^f/N). \tag{29}$$

To study the $N\to\infty$ limit, we shall separately consider the case $n^f=1$: for any given $n^f<1$, we obtain

$$\tilde{E}'_0=\tilde{E}_0=Dn^f\ , \tag{30}$$

$$Q'=Q=1-n^f\ , \tag{31}$$

$$\mu'=\mu=\tilde{E}_0-\tilde{D}\ , \tag{32}$$

thus confirming the statement of RS that the two methods give coincident results for $N\to\infty$.

The case $n^f=1$ is rather awkward: From Eq. (28) we obtain $\tilde{E}_0=D$ if we first take $N\to\infty$ and then $n^f\to 1$, but the result is $\tilde{E}_0=0$ if we reverse the order of the two limits. In the MFSB method we obtain instead the same result $\tilde{E}'_0=D$ when the limit is taken in the two ways. We shall prove that for $N\to\infty$ both the KB and MFSB methods give the same relevant physical quantity, namely, the ground-state energy E_g. From Eqs. (21) and (24), it is clear that

$$E_g\equiv\langle H\rangle=-(1-1/N)Q\tilde{E}_0=-Dn^f(1-n^f)\ , \tag{33}$$

while Newns and Read[7] find the expression [cf. their Eq. (124)]

$$E'_g=-(1-n^f)n^f(1-n^f/N)D=-Q'\tilde{E}'_0\ , \tag{34}$$

and therefore $E_g=E'_g$ in the limit $N\to\infty$.

It is clear that when $n=1$ all hopping is forbidden, and the ground-state energy should be zero for any value of N: this result follows from Eq. (33), because $Q=1/N$ and $\tilde{E}_0=0$, and from Eq. (34), because $Q'=0$ and $\tilde{E}'_0=D(1-1/N)$. To discuss this difference we note that in the MFSB method $\tilde{E}_0$ has two roles in the effective Hamiltonian [cf. Ref. 7, Eq. (110)]: (1) it shifts the center of the band to $\tilde{E}'_0$ and (2) it adds a constant term $\tilde{E}'_0(Q'-1)$ that compensates for the energy contribution of the band shift. One expects that for $n^f=1$ the shift of the band should be zero, because all hopping is forbidden, and the $\tilde{E}'_0$ shift derived in the MFSB method seems rather artificial, even if it is compensated by the constant term in the effective Hamiltonian. I therefore believe that the zero shift obtained by the KB method when $n=1$ gives a better description of the system.

To conclude, we may ask why the KB and MFSB methods give the same results (except for $n^f=1$) for the Hubbard model and different ones for the Anderson model, when $N\to\infty$. The basic reason is that the presence of the conduction band in the Anderson model allows variation of the n^f when the total number of electrons Nn^t is fixed, while in the Hubbard model we have a fixed $n^f=Nn^t$. As μ is determined by n^t, all the differences between the KB and MFSB methods go to zero when $N\to\infty$ (except for $n^f=1$) in the Hubbard model. In the Anderson model μ is determined by n^c+n^f/N, and in the limit $N\to\infty$ it is exclusively determined by n^c. In the Kondo region the E_f is far below μ, and to avoid $n^f>1$ the renormalized $\tilde{E}$ has to be very close to μ in the MFSB, while this condition is automatically satisfied in the KB. This aspect is more thoroughly discussed in Sec. V.

V. DISCUSSION

In this section we shall discuss why the KB functional expansion and the MFSB method give rather different results in the Kondo region. We shall concentrate on the simple model presented in Sec. III, but our conclusions are also valid in the general case.

The formulas for the KB method in Eqs. (20), differ explicitly from the corresponding ones in the MFSB method only by the presence of an extra factor Q in the expression for n^σ and a $(N-1)$ rather than N in that of $\tilde{E}$. A second difference is hidden in Q itself, because its actual expression differs in the two methods. These two differences have separate effects on the spectral densities, and we shall consider them one by one.

Consider first the factor $Q=(\tilde{V}/V)^2$, which determines the renormalization of the hybridization. In the KB method we have the same Eq. (25) as in the Hubbard method, while in the MFSB method we have $Q=1-n^f$ and in the Gutzwiller method $Q=(1-n^f)/(1-n^\sigma)$. All these expressions coincide in the $N\to\infty$ limit, but they are rather different for the Anderson model ($N=2$). For small n^σ the KB expression coincides with Gutzwiller's to $O|n^\sigma|$, but in the Kondo region, i.e., for $n^f\sim 1$, the KB value for $N=2$ is $Q\sim 0.5$, while in the two other methods it is $Q\sim 0$. When $Q\to 0$ (i.e., $\tilde{V}\to 0$), the gap tends to zero and the f spectral density $\rho^f(\omega)$ becomes a δ function at $\tilde{E}$. In the KB the minimum is $Q=0.5$, and so the hybridization is not canceled in the Kondo region and the spectral density has instead an appreciable width.

Let us now consider the second difference, namely, the presence of an extra Q in the KB expression for n^σ [cf. Eq. (20)]. This extra factor was already attributed in Sec. III to the fact that the GF with Hubbard operators X describes correlated electrons, in contrast to the band of uncorrelated electrons of the "effective Hamiltonian" treatments. The integrated spectral intensity per channel is Q for the KB method, while it is 1 for the MFSB method, and as a consequence, the relation $n^f\le 1$ is automatically satisfied in the KB method, even when $\tilde{E}$ is far below μ: The resulting energy renormalization $\tilde{E}-E_f$ is even then only moderate. To satisfy $n^f\le 1$ in the MFSB method,

the μ has to be in the lower band for E_f sufficiently low and therefore $\tilde{E} > \mu$ because $\tilde{E}$ is always in the gap. When $n^t > 1/N$ we need at least $n^t - 1/N$ conduction electrons, so that μ has also a minimum value independent of E_f, as shown in Figs. 1(c), 2(a), and 2(c). In that case $\tilde{E} - E_f > \mu - E_f$ can be rather large when E_f is well below μ, as shown in the same figures. It is clear that this large renormalization of the MFSB method is only a consequence of the restrains that have to be imposed on the otherwise uncorrelated band of electrons. At first sight this large renormalization seems rather unphysical, but we shall see below that it is necessary in the "effective Hamiltonian" techniques to describe an important aspect of the problem. From the considerations presented above, it follows that the difference between the KB and MFSB expressions for both n^σ and Q have separate effects in the Kondo limit: (1) The difference between the two expressions of Q gives a peak of a much larger width in the KB versus MFSB methods. (2) The difference in the expression of n^σ gives a much smaller energy renormalization $\tilde{E} - E_f$ in the KB versus MFSB methods.

At this point it is interesting to compare the KB and MFSB results with those that Brandow[11] obtained by a variational method (BVM) that imposes correlation directly into the trial wave function. In his simplest one-parameter theory, he finds a quasiparticle spectrum of the same form obtained in the MFSB method, and with energy and hybridization renormalizations consistent with those of that theory. The spectral density $\rho^f(\omega)$ is concentrated around a renormalized energy $\tilde{\varepsilon}$ and consists of two sharp peaks separated by a gap, but with a total f spectral intensity of $1 - n^f$, i.e., a rather drastic reduction of the MFSB spectral intensity of 1. At the same time he states that there is also a nonquasiparticle contribution to ρ^f, and based on the formal similarity to the single-impurity case, he conjectures that this contribution should be a broad peak centered near E_f.

The BVM as well as the different "effective Hamiltonian" theories are variational in nature, and they should give the best possible description of the free energy, compatible with the approximation. When $n^f \sim 1$ all these variational techniques show a peak of $\rho^f(\omega)$ close to μ, which strongly modifies the thermodynamic properties of the system at low T. As stated by Brandow, "this peak has, apart from the gap near its center, all the qualitative features of the so called Kondo peak." The absence of this structure should therefore make the KB approximation worse than the variational ones with regard to the thermodynamic properties. On the other hand, the BVM shows that most of the f spectral weight is outside this region (when $n^f \sim 1$) and, probably, in the form of a wide structure around E_f, just like in the KB expansion. My conclusion from these facts is that in the region of $n^f \sim 1$ the KB and MFSB theories give complementary aspects of the f spectral function: The spectral density is represented by the sum of the ρ^f derived from both methods, with the MFSB spectral density reduced by a factor $1 - n^f$ and therefore giving only a negligible contribution to n^σ. It was already stated above that both theories are qualitatively similar outside the region of $n^f \sim 1$.

We should also mention that the two peaks around $\tilde{E}$ obtained in BVM were also found by Grewe[14] by employing the same type of GF with Hubbard operators of the present work. He uses at each site the single-impurity GF calculated in the noncrossing approximation and connecting all the sites with unperturbed GF of conduction electrons, but adding a self-exclusion term to avoid overcounting processes already considered in the single-impurity GF. In the exactly soluable case of a lattice of resonant levels, he finds that the pole of the impurity GF that produces a Lorentzian density of states is exactly canceled. The lattice of resonant levels is described in our model by a system with a single channel, and our treatment gives an exact solution, with the same cancellation discussed by Grewe. In the correlated case he finds only a pseudogap, and he cannot definitely conclude that the Kondo lattice possesses a real gap at $T = 0$ K.

The results of the different methods discussed above leave little doubt that when $n^f \sim 1$ and $T \to 0$ K there should be a structure of $\rho^f(\omega)$ around μ, probably with a gap or pseudogap. This structure is absent in our approximation, but I believe that it should appear in a higher-order calculation.

Another result that deserves further comment is the maximum of $\rho^F \equiv \rho^f(\mu)$ observed in the KB approximation when $n^t > 1/N$. This structure was explained in Sec. III and gives a distorted picture of the $\rho^f(\omega)$ when μ sweeps through the values of ω. The shape of $\rho^f(\omega)$ is deformed because also the renormalized $\tilde{E}$ and $\tilde{V}$ depend on the value of μ. In our theory there is only one broad structure, centered at an $\tilde{E}$ not very far from E_f, and it is then clear why the maximum of ρ^F coincides with the region of *IV*. The negligible value obtained in our method for ρ^E in the Kondo region points out the main deficiency of the KB approximation, namely, the corresponding lack of a structure of $\rho^f(\omega)$ close to the chemical potential μ. As discussed before, the MFSB method gives just that structure and only that, when $n^f \sim 1$, and it is therefore clear why the ρ^F curves are so different in the KB versus MFSB theories [cf. Figs. 1(b) and 2(b) where the two ρ^F have been plotted].

It is also interesting to consider the single-impurity case. The modifications to the calculation are straightforward, and one obtains

$$G(\sigma, fj, fj/z) = Q[z - \tilde{E} - |\tilde{V}|^2 F_0(z)]^{-1} , \tag{35}$$

where

$$F_0(z) = (1/N_s) \sum_{\mathbf{k}} [z - E(\mathbf{k}, \sigma)]^{-1}, \tag{36}$$

and $\tilde{E}$, Q, and $|\tilde{V}|^2$ are given by the same Eqs. (14)–(16).

For the simple model of Sec. III, we find

$$F(\omega + i0) = \rho_0 \{ \ln[(D + \omega)/(D - \omega)] - i\pi \}, \tag{37}$$

and the real part can be neglected when $\omega/D \ll 1$, i.e., for frequencies ω far from the ends of the conduction band. We shall then use $F(\omega + i0) \sim -i\pi\rho_0$, and from Eq. (35) we find

$$\rho^f_\sigma(\omega) = (Q/\pi) \tilde{\Delta} [(\omega - \tilde{E})^2 + \tilde{\Delta}^2]^{-1} , \tag{38}$$

with $\tilde{\Delta} = Q\Delta$ and $\Delta = \pi\rho_0 V^2$. The relation between the

MFSB and KB calculations for the impurity is the same found for the lattice: The only difference is the actual expression of Q and an extra factor Q in the expression of n^σ. In the KB method we find, at $T=0$ K,

$$n^\sigma=(1/\pi)Q\{\tan^{-1}[(\mu-\tilde{E})/\tilde{\Delta}] - \tan^{-1}[-(D+\tilde{E})/\tilde{\Delta}]\} . \quad (39)$$

The chemical potential μ does not depend on n^σ and is given by

$$\mu=D(2n^t-1) . \quad (40)$$

If we apply Friedel's rule to this problem,[15] we can write

$$\rho^F=\rho^f(\mu)=(1/\pi\Delta)\sin^2(\pi n^f/N) . \quad (41)$$

We can now introduce n^σ from Eq. (39) into Eq. (41) and compare with Eq. (38) for $\omega=\mu$ given by Eq. (40).

Let us first consider the case of $n^0 \ll 1$: We find $\rho^F=[\pi(n_\sigma^2)/\Delta](1+O|n^\sigma|)$, so that Friedel's rule is very well satisfied in this limit. As the spectral density $\rho^f(\omega)$ is a Lorentzian centered at $\tilde{E}$, the Kondo peak is absent in the $n^f \sim 1$ limit, where Friedel's rule gives $\rho^F \sim 1/\pi\Delta$ for the Anderson model [cf. Eq. (41) for $N=2$]. As in the lattice case, the KB treatment gives $\mu-\tilde{E} \gg \tilde{\Delta}$ for the impurity, and Friedel's rule is not satisfied because then $\rho^F \ll 1/\pi\Delta$. It is interesting to note that it is only the presence of Q in n^σ [Eq. (39)] and not its actual value that gives this result by making $\mu-\tilde{E} \gg \tilde{\Delta}$. It is obvious from Eq. (38) that Q cancels out when $\tilde{E} \sim \mu$, as in the MFSB case, and the $\rho^F=1/\pi\Delta$ that satisfies Friedel's rule is then obtained for any value of Q.

In the MFSB case the low-temperature thermodynamic properties are optimized by the variational method, and the whole spectral density described by a broad Lorentzian is deformed and shifted so that it would mimic the Kondo resonance. Between the two limits of n^σ the KB calculation gives increasing accord with Friedel's sum rule when n^σ decreases toward $n^\sigma \ll 1$.

In the present work we have not studied the stability of the paramagnetic phase against other magnetic phases; nor have we calculated thermodynamic properties: Consideration of these topics and the inclusion of higher-order approximations is under way.

[1] J. Hubbard, Proc. R. Soc. London, Ser. A **276**, 238 (1964); **281**, 401 (1965): These are two in a series of six papers.

[2] A. C. Hewson and A. L. Wasserman, J. Phys. **1**, 403 (1989); A. J. Fedro and B. D. Dunlap, Jpn. J. Appl. Phys. **26**, DL04 (1987).

[3] H. Keiter and G. Morandi, Phys. Rep. **109**, 227 (1984).

[4] C. M. Varma, W. Weber, and L. J. Randall, Phys. Rev. B **33**, 1015 (1986); P. Fazekas and B. H. Brandow, Phys. Scr. **36**, 809 (1987).

[5] S. E. Barnes, J. Phys. F **6**, 1375 (1976); **7**, 2637 (1977); P. Coleman, Phys. Rev. B **29**, 3035 (1984).

[6] N. E. Bickers, Rev. Mod. Phys. **59**, 845 (1987).

[7] D. M. Newns and N. Read, Adv. Phys. **36**, 799 (1987); Solid State Commun. **52**, 993 (1984).

[8] G. Kotliar and A. E. Ruckenstein, Phys. Rev. Lett. **57**, 1362 (1986).

[9] A. E. Ruckenstein and S. Schmitt-Rink, Phys. Rev. B **38**, 7188 (1988).

[10] L. P. Kadanoff and G. Baym, *Quantum Statistical Mechanics* (Benjamin, New York, 1962).

[11] B. H. Brandow, Phys. Rev. B **33**, 215 (1986).

[12] P. A. Lee, T. M. Rice, J. W. Serene, L. J. Sham, and J. W. Wilkins, Comments Condens. Matter Phys. **12**, 99 (1986).

[13] G. Czycholl, Phys. Rep. **143**, 277 (1986); Eq. (7.18).

[14] N. Grewe, Solid State Commun. **50**, 19 (1984). The following works explore further the same approach: N. Grewe, Z. Phys. B **67**, 323 (1987) and N. Grewe, T. Prushke, and H. Keiter, *ibid.* **71**, 75 (1988).

[15] G. Gruner and A. Sawadowski, Rep. Prog. Phys. **37**, 1497 (1974); O. Günnarsson and K. Schönhamer, Phys. Rev. Lett. **50**, 604 (1983).